Journal of Alloys and Compounds 609 (2014) 185–191

Contents lists available at ScienceDirect

Journal of Alloys and Compounds

journal homepage: www.elsevier.com/locate/jalcom

Structural phase transformations and new intermediate phases of MgF_2 under high-pressures applied via conjugate-gradient method

Hülya Öztürk *, Cemile Kürkçü, Cihan Kürkçü

Fizik Bölümü, Ahi Evran Üniversitesi, Kırşehir 40100, Turkey

ARTICLE INFO

Article history:
Received 18 March 2014
Received in revised form 18 April 2014
Accepted 21 April 2014
Available online 30 April 2014

Keywords:
Magnesium fluoride
Intermediate phase
Phase transformation
Molecular dynamics

ABSTRACT

An ab initio constant pressure technique is performed in order to study the structural behavior of MgF_2 under the hydrostatic pressure up to 700 GPa. Two high-pressure phases of MgF_2 are successfully observed through constant pressure simulations. MgF_2 undergoes a phase transformation from the rutile-type structure to the cubic-fluorite-type structure with space group $Fm\bar{3}m$ at 280 GPa. Another phase transformation from the cubic-fluorite-type structure to the cotunnite-type structure with space group *Pnma* occurs at 500 GPa. The first transformation proceeds via three intermediate phases with space groups *Pnnm*, *Immm* and $R\bar{3}m$. We also investigate the stability of these phases from the total energy and enthalpy computations. According to these investigations, the phase transformations should occur from the rutile-type structure to the cubic-fluorite-type structure around 20 GPa and from the cubic-fluorite-type structure to the cotunnite-type structure around 45 GPa.

1. Introduction

The lattice dynamics of MgF_2 have been studied for the first time by Katiyar and Krishnan, using a rigid ion model with short-range central axially symmetric forces and long-range Coulomb forces [1]. Because of technological properties and academic importance of this material, many studies on structural, thermodynamic and optical behaviors [2–4], elastic properties, band structures, chemical bonding [5–7], energy landscapes and temperature driven phase changes [8–10], high-pressure behaviors [11–15] of this material have been performed.

Although MgF_2 crystallizes in a similar way of transition metal compounds of BF_2-type in a tetragonal rutile-type structure with space group $P4_2/mnm$ at ambient conditions, *Mg* is not a transition metal. Lack of d-electrons and the greatly ionic character of magnesium fluoride simplify the theoretical studies. Thanks to the higher compressibility of MgF_2 and relative sizes of its ions, the phase transformations of this material are found at lower pressures than those in many dioxides. These phase changes can be investigated under hydrostatic or nearly hydrostatic circumstances.

The high-pressure behavior of MgF_2 is reasonably curious. Whereas some studies [11–13] and our recent study [15] applying Parrinello and Rahman method give emphasis to that the tetragonal rutile-type MgF_2 should be transformed into an orthorhombic $CaCl_2$-type structure with space group *Pnnm*, some other studies [16–21] underline that this material should be transformed into a cubic-fluorite-type structure with space group $Fm\bar{3}m$ at high pressures. The results of this study applying conjugate-gradient method support the later transformation; that is, this study underlines that the tetragonal rutile-type MgF_2 should be transformed into a cubic-fluorite-type structure with space group $Fm\bar{3}m$ at high pressure. According to the results of this study, sequence of the stable phases of MgF_2 has been found as $P4_2/mnm \rightarrow Fm\bar{3}m \rightarrow Pnma$.

The particular structural features of the transition or the transition mechanism are still not known owing to difficulties in mapping out the atomistic motions while carrying out the experiments. In the present work, we suggest a simulation study of the transformation mechanism of MgF_2. We propose the cubic-fluorite-type structure of this substance with space group $Fm\bar{3}m$ proceeds through three intermediate phases with space groups *Pnnm*, *Immm* and $R\bar{3}m$, expressed as MgF_2 – (*a*), MgF_2 – (*b*) and MgF_2 – (*c*), respectively. As far as we know, these intermediary phases have not been obtained in any previous studies. Although an orthorhombic $CaCl_2$-type structure with space group *Pnnm* has been obtained as a stable phase in some previous studies [11–13] and our recent study [15] applying Parrinello and Rahman method, an intermediate phase expressed as MgF_2 – (*a*) with the same space group *Pnnm* is estimated in this study using conjugate-gradient method.

* Corresponding author. Tel.: +90 386 2804555; fax: +90 386 2804525.
E-mail addresses: hozturk@ahievran.edu.tr, hulyaozturk@gazi.edu.tr (H. Öztürk).

http://dx.doi.org/10.1016/j.jallcom.2014.04.152
0925-8388/

2. Computational details

The density functional calculations were carried out within the generalized gradient approximation (GGA) [22] using the ab initio program SIESTA [23]. A localized linear combination of atomic orbital basis sets was considered to describe valence electrons and norm-conserving nonlocal pseudopotentials of atomic core. Troullier–Martins schemes [24] were used in order to establish norm-conservative pseudopotentials. Double-ζ plus polarized basis sets were applied. A uniform mesh with a plane wave cut-off of 150 Ry was used with the aim of representation of the electron density, the local part of the pseudopotentials, the Hartree and the exchange-correlation potential. A simulation cell of 96 atoms was chosen and the periodic boundary conditions were applied. Γ-point sampling was employed for the Brillouin zone integration.

We used conjugate-gradient method to apply pressure to the system. The system was relaxed at zero pressure and then pressure was gradually increased. This approach has already been used successfully in predicting a series of pressure-induced structural phase transitions of various compounds [25–30]. For each value of the applied pressure, the structures were allowed to relax and find their equilibrium volumes and their lowest energies by optimizing their lattice vectors and atomic positions together until the maximum atomic forces were smaller than 0.01 eV $Å^{-1}$ and the stress tolerances were less than 0.5 GPa. We used the RGS algorithm and the KPLOT program [31,32] that allow detailed information about a given structure such as space group, cell parameters and atomic positions to identify symmetries of the phases observed in the simulations.

We take the energy–volume computations into account to study the stability of high-pressure phases of MgF_2 since transition pressures obtained in constant-pressure simulations are generally overestimated. In order to compute energy volumes, we used the unit cells for the $P4_2/mnm$, $Fm\bar{3}m$ and *Pnma* high-pressure phases. The Brillouin zone integration was performed with an automatically produced 6-6-6 k-point mesh for the phases prepared according to the method of Monkhorst and Pack [33]. The obtained total energy–volume dependences were fitted to the third-order Birch–Murnaghan equation of states [34,35]. Enthalpy calculations give usually realistic transition pressures compared with experiments. Since the phase transitions occur at the same enthalpy of the two phases, the transition pressure can be easily obtained by equating the enthalpy of the two phases.

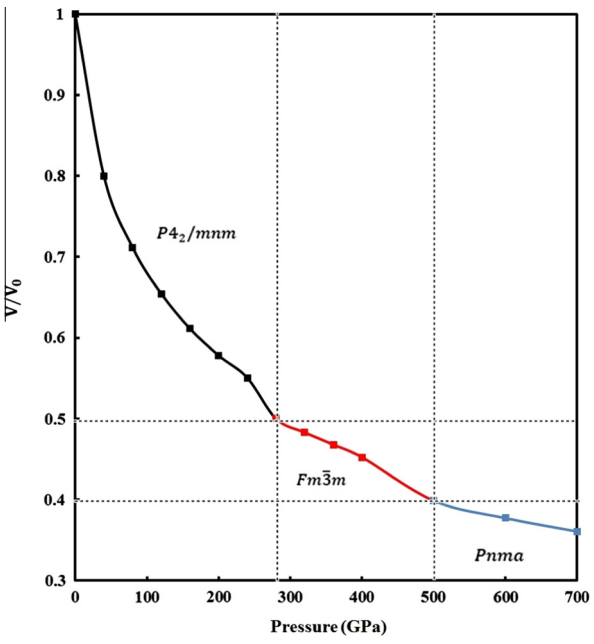

Fig. 1. The volume change of the simulation cell as function of pressure.

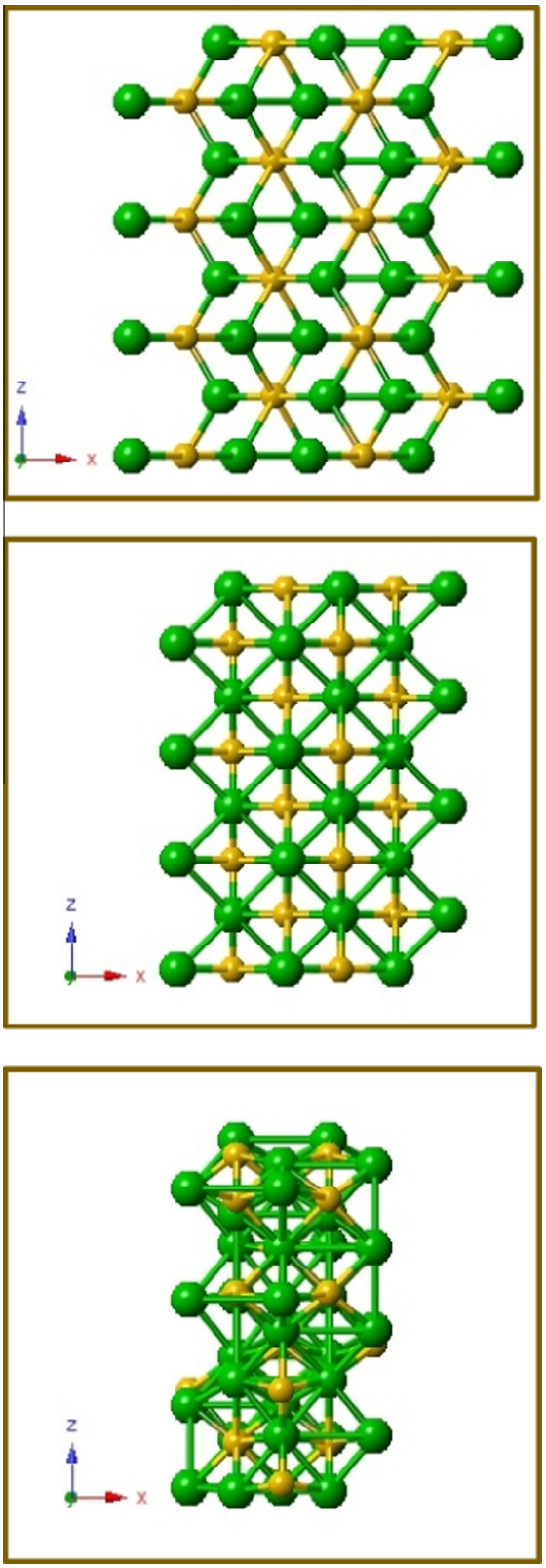

Fig. 2. Crystal structures of MgF_2: $P4_2/mnm$ (first panel) at zero pressure, $Fm\bar{3}m$ (second panel) at 280 GPa and *Pnma* (third panel) at 500 GPa.

3. Results and discussions

In order to identify the thermodynamic nature of the phase transitions in MgF_2, the pressure–volume dependence of this material are investigated and illustrated in Fig. 1. As seen from this figure, the volume decreases monotonically and indicates the phase transitions at 280 GPa and 500 GPa. Unsurprisingly, the rutile-type structure transforms to the cubic-fluorite-type structure with space group $Fm\bar{3}m$ at 280 GPa and this cubic-fluorite-type structure transforms to the cotunnite-type structure with space group *Pnma* at 500 GPa. These structures are shown in Fig. 2. The pressure has been increased up to 700 GPa in order to explore whether there are another phase transformations or not.

Despite the increasing pressure, the rutile-type structure is still conserved up to 240 GPa. Once the applied pressure is increased from 240 to 280 GPa, the structural transition emerges together with by a dramatic volume decrease of the simulation cell. At 280 GPa, the rutile-type structure transforms into the cubic-fluorite-type structure in agreement with the literature [17–20]. We carefully analyzed this structure at each minimization step via the KPLOT program to examine whether there are any intermediate phases during this phase transformation or not. We obtain an orthorhombic structure expressed as MgF_2 – (*a*) having *Pnnm* symmetry at 289 minimization step, another orthorhombic structure expressed as MgF_2 – (*b*) having *Immm* symmetry at 323 Step and also a trigonal structure expressed as MgF_2 – (*c*) having $R\bar{3}m$ symmetry at 324 Step. These intermediary phases are illustrated in Fig. 3. The MgF_2 – (*b*) and the MgF_2 – (*c*) structures are also obtained from 325 to 330 Steps and from 331 to 337 Steps, respectively. The cubic-fluorite-type structure having $Fm\bar{3}m$ symmetry forms at 338 minimization step.

The volume shows a small discontinuity at 500 GPa. This discontinuity indicates another phase transition. At this pressure, the cubic-fluorite-type structure transforms into the cotunnite-type structure with space group *Pnma*, in agreement with the literature [11,12]. This structure is denser than α-$PbCl_2$-type structure having the same *Pnma* symmetry obtained in our recent study [15] using Parrinello and Rahman method. Although we analyzed this structure at each minimization step using the KPLOT program, we did not find any intermediate state.

We have studied the atomic movements during the phase transformations to elucidate the mechanism of phase transitions. The simulation cell vector lengths and angles have been plotted in Fig. 4 as a function of minimization steps at 280 and 500 GPa pressures. These cell vectors stated as **A**, **B**, and **C** are initially along the [100], [010] and [001] directions, correspondingly.

Transition pressures obtained in constant-pressure simulations are usually overvalued. When the particular conditions such as the lack of any defect in simulation cells and finite size of these cells are considered, such overvalued transition pressures are predicted. Structural phase transformations in simulations do not progress by nucleation and growth, as a substitute they occur across the entire simulation cells. Thus, systems have to cross a noteworthy energy barrier to transform from one phase to another one, and from this time simulated structures have to be overpressed in order to get a phase transformation [36,37]. In addition, the lack of thermal motion in our simulations moves the phase transformations to higher pressures. Conversely, the thermodynamic theorem does

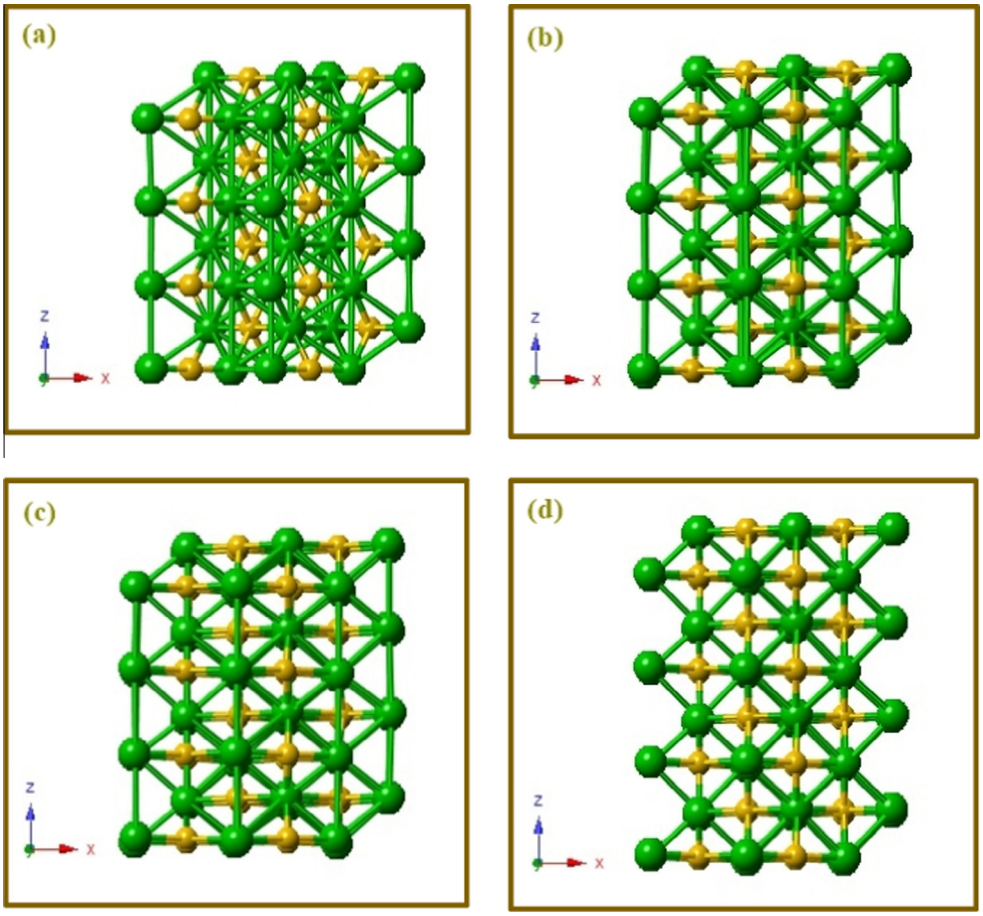

Fig. 3. At 280 GPa, evolution of the cubic-fluorite-type structure at minimization steps: (a) 289 Step, (b) 323 Step, (c) 324 Step and (d) 338 Step.

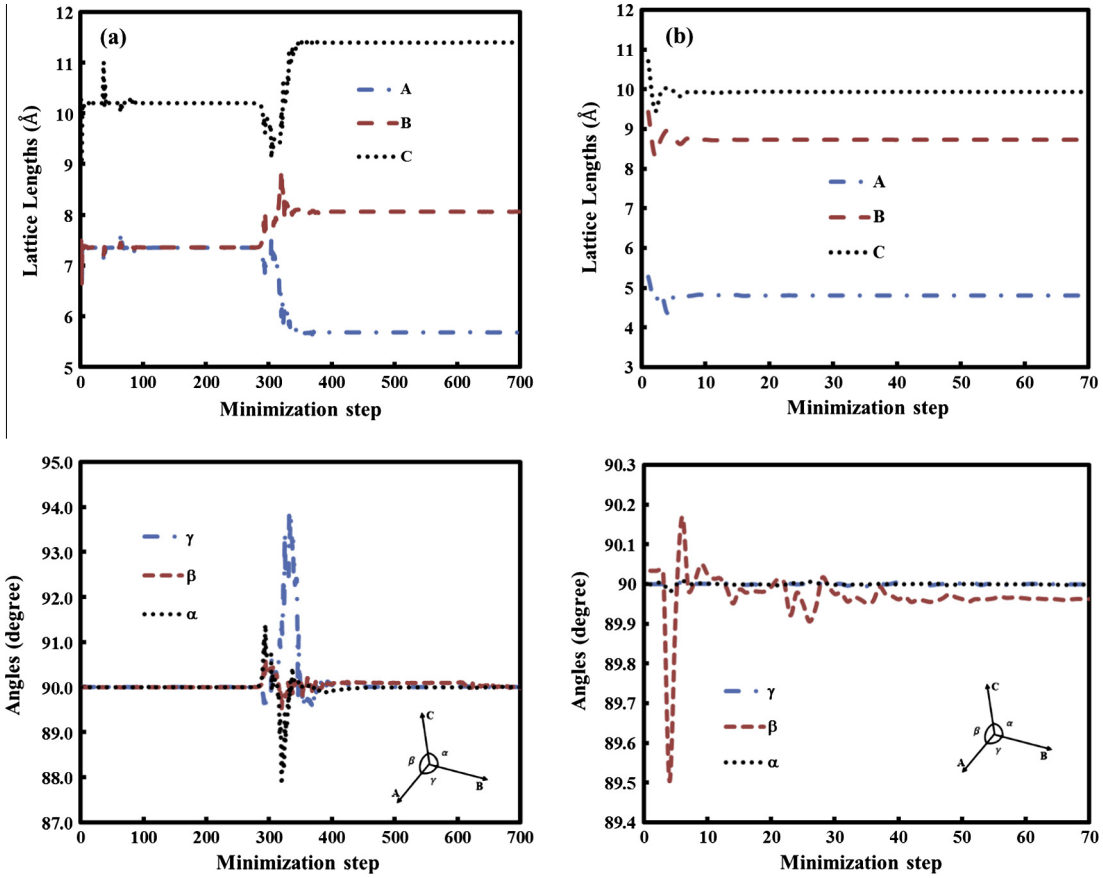

Fig. 4. The behavior of the simulation cell lengths and angles as function of minimization steps (a) at 280 GPa and (b) at 500 GPa.

not take into account the thermal motion and the probable existence of an activation barrier separating the two structural phases. For that reason, as a next step, we think the energy–volume calculations to study the stability of high-pressures phases of MgF_2. Since intermediate phases are not stable, there is no benefit of the application of this approach for the intermediate phases participating the first high-pressure phase transition at 280 GPa.

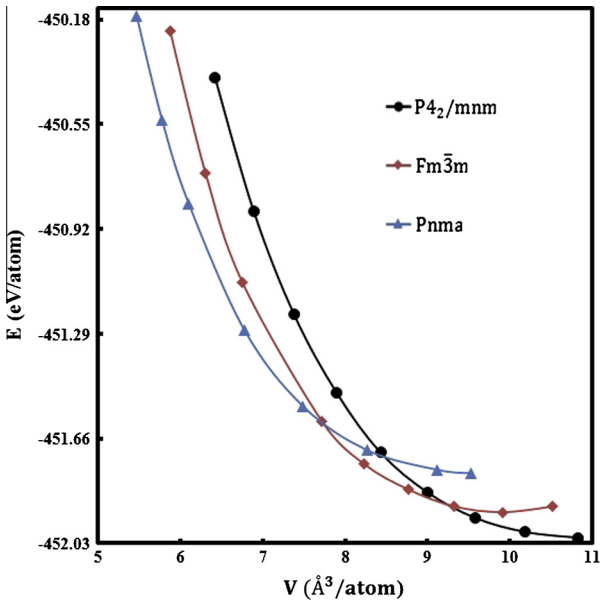

Fig. 5. The energy–volume curves of main structural phases of MgF_2.

Table 1
Transition pressures (P), equilibrium volumes (V), the bulk modules (B_0) and their pressure derivatives (B_0') and equilibrium lattice parameters (a, b and c) of MgF_2 phases.

Phase	Reference	P (GPa)	V (Å^3)	B_0 (GPa)	B_0'	a (Å)	b (Å)	c (Å)
$P4_2/mnm$	This study	0	32.48	116	4.32	4.6072	4.6072	3.0770
	[9]					4.6080	4.6080	3.0070
	[11]			98	3.70	4.6249	4.6249	3.0520
	[11] (Expt.)			101	4.20	4.6213	4.6213	3.0519
	[11] (Expt.)					4.6280	4.6280	3.0450
	[12]			101		4.5720	4.5720	3.0170
	[12] (Expt.)			101		4.6250	4.6250	3.0520
	[38]			97	3.70	4.6912	4.6912	3.0960
$Fm\bar{3}m$	This study	20	29.71	137.03	4.14	4.0273	4.0273	4.0273
	[14] (GGA)			106.1	4.08	5.0440	5.0440	5.0440
	[14] (LDA)			128.8	4.02	4.9050	4.9050	4.9050
	[17] (Expt.)	30						
	[18]	23						
	[19] (Expt.)	25				4.7920	4.7920	4.7920
	[20] (Expt.)			107.5		4.9310	4.9310	4.9310
	[20] (Expt.)					4.9400	4.9400	4.9400
$Pnma$	This study	45	26.88	155	4.05	4.3656	2.4027	9.9284
	[11]	38		158	3.50			
	[11] (Expt.)			163	7			
	[12]	36.8		259		5.1040	5.7160	3.0450
	[12] (Expt.)			163				

We have drawn the total energy as a function of volume depicted in Fig. 5 and presented the equilibrium volumes, lattice parameters, bulk modules and their pressure derivatives in Table 1. As seen in the table, this study gives comparable results with

experiments and theoretical calculations. In order to decide the most stable structure at finite pressure and temperature, the free energy $G = E_{tot} + PV - TS$ should be used. In this study, density functional calculations are essentially achieved at zero temperature and the TS term is neglected. Thus, the enthalpy, $H = E_{tot} + PV$ including the pressure–volume effects is obtained. Since at the phase transition the two phases require the same enthalpy, the transition pressure can be simply predicted by equating the enthalpy of the two phases. We have calculated the enthalpies via the energy–volume data and plotted them in Fig. 6 as a function of pressure. The intersection of two enthalpy curves indicates a phase transition between two phases. The enthalpy curve of $P4_2/mnm$ phase crosses with that of the $Fm\bar{3}m$ phase at about 20 GPa. Thus, we can say that a first-order phase transition occurs between $P4_2/mnm$ and the $Fm\bar{3}m$ phases at this pressure. The $Fm\bar{3}m$ phase has already been obtained by Allan et al. at 23 GPa [18] theoretically and by Ming and Manghnani at 30 GPa [17] and Nishidate et al. at 25 GPa [19] experimentally. The enthalpy curve of this phase crosses with that of the *Pnma* phase at about 45 GPa, indicating also a first-order phase transition between this and *Pnma* phases. The *Pnma* phase has already been obtained both

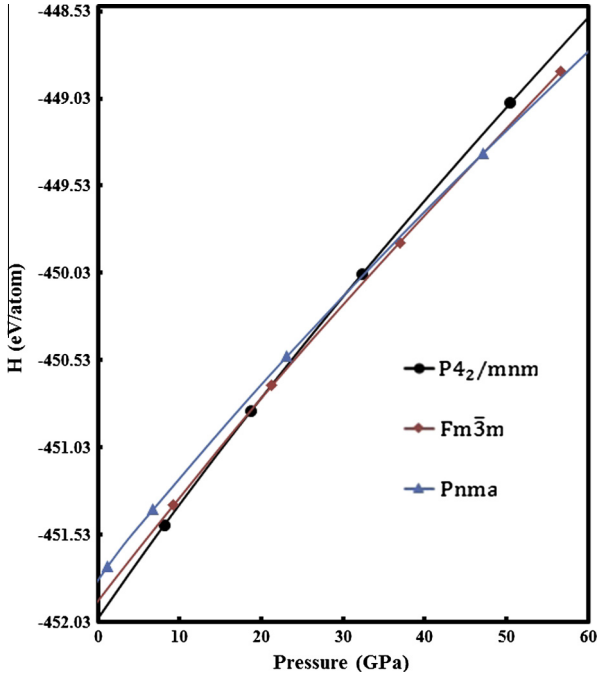

Fig. 6. The enthalpy curves of main structural phases of MgF_2 as function of volume.

Table 2
The bond lengths with minimum and maximum values and coordination numbers of the $P4_2/mnm$, $Fm\bar{3}m$, *Pnma*, *Pnnm*, *Immm* and $R\bar{3}m$ phases. B_{min} and B_{max} indicate minimum and maximum bond lengths, respectively.

Phase	From	To	B_{min} (Å)	B_{max} (Å)	Coordination
$P4_2/mnm$	F	Mg	1.984	1.998	$F \Rightarrow [1–3]Mg$ $Mg \Rightarrow [2–6]F$
	F	F	2.548	2.548	$F \Rightarrow [0–1]F$
$Fm\bar{3}m$	F	Mg	1.742	1.746	$F \Rightarrow [1–4]Mg$ $Mg \Rightarrow [3–7]F$
	F	F	2.009	2.018	$F \Rightarrow [0–6]F$
Pnma	F	Mg	1.611	1.871	$F \Rightarrow [1–5]Mg$ $Mg \Rightarrow [2–9]F$
	F	F	1.864	2.403	$F \Rightarrow [1–11]F$
Pnnm	F	Mg	1.470	1.698	$F \Rightarrow [1–3]Mg$ $Mg \Rightarrow [2–6]F$
	F	F	2.080	2.535	$F \Rightarrow [1–12]F$
Immm	F	Mg	1.659	2.028	$F \Rightarrow [1–4]Mg$ $Mg \Rightarrow [3–7]F$
	F	F	1.858	2.736	$F \Rightarrow [1–8]F$
$R\bar{3}m$	F	Mg	1.582	1.931	$F \Rightarrow [1–4]Mg$ $Mg \Rightarrow [3–7]F$
	F	F	1.788	2.737	$F \Rightarrow [1–9]F$

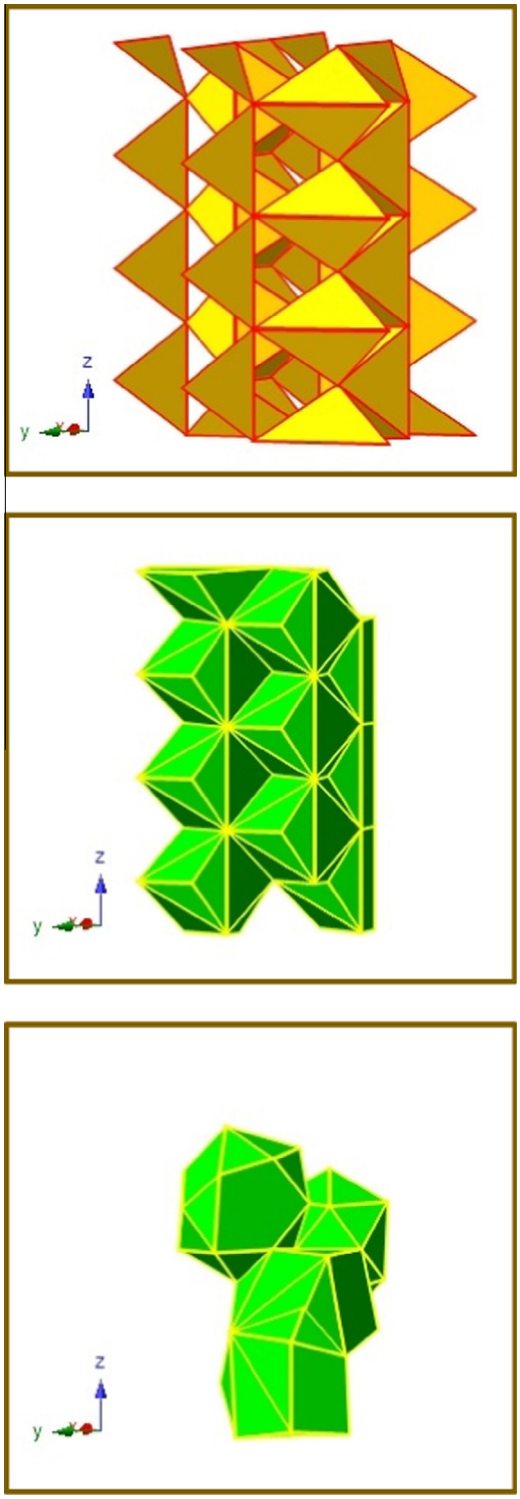

Fig. 7. Polyhedral views of MgF_2 structures: $P4_2/mnm$ (first panel) at zero pressure, $Fm\bar{3}m$ (second panel) at 280 GPa and *Pnma* (third panel) at 500 GPa.

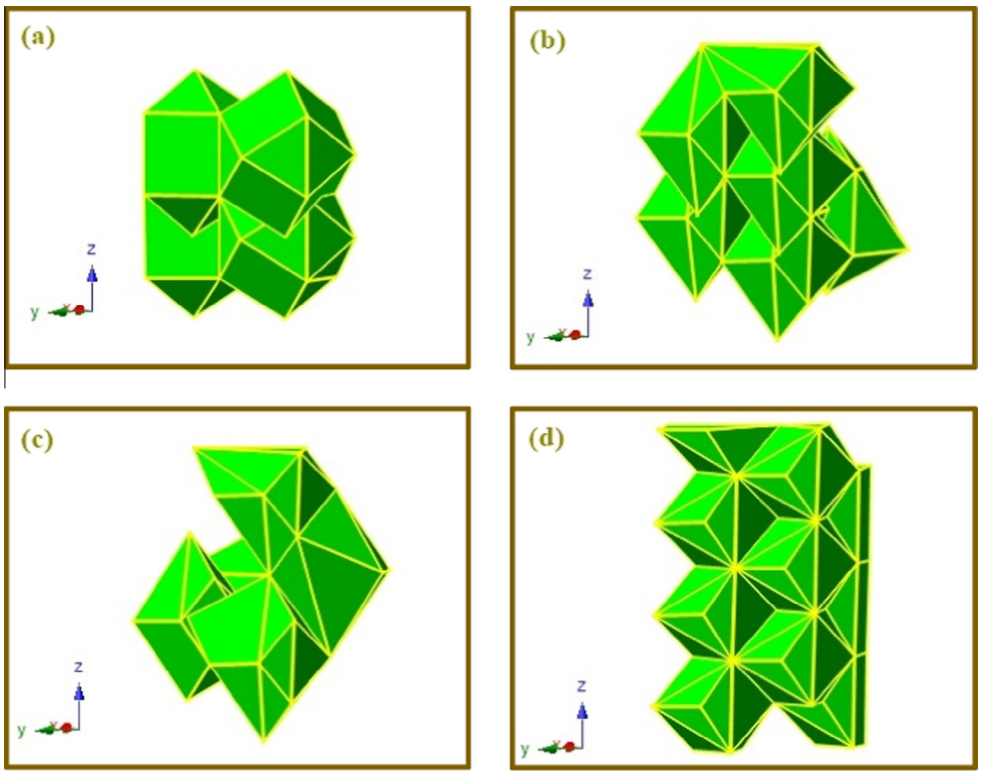

Fig. 8. At 280 GPa, polyhedral views of MgF_2 structures obtained at minimization steps: (a) MgF_2 – (*a*) at Step 289, (b) MgF_2 – (*b*) at Step 323, (c) MgF_2 – (*c*) at Step 324 and (d) MgF_2 – (*d*) at Step 338.

experimentally and theoretically Haines et al. at 38 GPa [11] and Kanchana et al. at 36.8 GPa [12].

Mg is six-, seven- and nine-fold coordinated by *F* for the rutile-type structure, the cubic-fluorite-type structure and the cotunnite-type structure, respectively. The *Mg–F* bond lengths range from 1.984 to 1.998 Å and the *F–F* bond lengths are 2.548 Å for the rutile-type structure. The *Mg–F* bond lengths range from 1.742 to 1.746 Å and the *F–F* bond lengths range from 2.009 to 2.018 Å for the cubic-fluorite-type structure. The *Mg–F* bond lengths range from 1.611 to 1.871 Å and the *F–F* bond lengths range from 1.864 to 2.403 Å for the cotunnite-type structure. The *Mg* is six-, seven-, and seven-fold coordinated by *F* for MgF_2 – (*a*), MgF_2 – (*b*) and MgF_2 – (*c*), respectively. The *F* is three-, four- and four-fold coordinated by *Mg* for MgF_2 – (*a*), MgF_2 – (*b*) and MgF_2 – (*c*), respectively. The *Mg–F* bond lengths range from 1.470 to 1.698 Å and the *F–F* bond lengths range from 2.080 to 2.535 Å for MgF_2 – (*a*). The *Mg–F* bond lengths range from 1.659 to 2.028 Å and the *F–F* bond lengths range from 1.858 to 2.736 Å for MgF_2 – (*b*). The *Mg–F* bond lengths range from 1.582 to 1.931 Å and the *F–F* bond lengths range from 1.788 to 2.737 Å for MgF_2 – (*c*). The bond lengths with minimum and maximum values and coordination numbers of the $P4_2/mnm$, $Fm\bar{3}m$, *Pnma*, *Pnnm*, *Immm* and $R\bar{3}m$ phases are summarized in Table 2. The polyhedral structures of these phases are illustrated in Figs. 7 and 8.

The results of this study are comparable with experimental and theoretical values. We can conclude from the enthalpy curves that the first phase transition from the $P4_2/mnm$ phase to the $Fm\bar{3}m$ phase occurs at about 20 GPa, which is comparable with the literature results [17–20] ranging from 10 to 40 GPa and the second phase transition from the $Fm\bar{3}m$ phase to the *Pnma* phase occurs at about 45 GPa, which is comparable with the literature results [11,12,38]. Thus, we suppose to see these phase transitions in experiments about these pressures.

4. Conclusions

The response of MgF_2 to hydrostatic pressures has been studied using ab initio constant pressure simulations and observed two high-pressure phases and three intermediate phases in the simulations. These high-pressure phases agree with the results of some earlier studies, but the intermediate phases obtained in this study have not been observed in any other previous studies. The phase transition from the rutile-type structure to the cubic-fluorite-type structure is based on these three intermediate phases with space groups *Pnnm*, *Immm* and $R\bar{3}m$. These results let different perspectives on the transformation mechanism of the rutile-type structure to the cubic-fluorite-type structure phase transition. Trustworthy dynamical simulations are needed owing to the difficulties in working out the atomistic motions while performing the experiments.

Acknowledgement

This study was supported by the Ahi Evran University under Scientific Research Project (BAP) No.: FBA-10-14.

References

[1] R.S. Katıyar, R.S. Krıshnan, Can. J. Phys. 45 (1967) 3079–3090.
[2] C. Muhlhausen, R. Gordon, Phys. Rev. B 23 (1981) 900–923.
[3] K.R. Babu, Ch.B. Lingam, S. Auluck, S.P. Tewari, G. Vaitheeswaran, J. Solid State Chem. 184 (2011) 343–350.
[4] A. Duncanson, R.W.H. Stevensen, Proc. Phys. Soc. 72 (1958) 1001–1006.
[5] M. Catti, A. Pavese, R. Dovesi, C. Roetti, M. Causa, Phys. Rev. B 44 (1991) 3509–3517.
[6] J.K. Vassiliou, J. Appl. Phys. 57 (1985) 4543–4547.
[7] W.H. Baur, Acta Crystallogr. B 32 (1976) 2200–2204.
[8] M.A.C. Wevers, J.C. Schön, M. Jansen, J. Solid State Chem. 136 (1998) 233–246.
[9] M.A.C. Wevers, J.C. Schön, M. Jansen, J. Phys.: Condens. Matter 11 (1999) 6487–6499.

[10] K.H. Hoffmann, J.C. Schön, Eur. Phys. J. B 86 (2013) 220–229.
[11] J. Haines, J.M. Leger, F. Gorelli, D.D. Klug, J.S. Tse, Z.Q. Li, Phys. Rev. B 64 (2001). 134110-1-10.
[12] V. Kanchana, G. Vaitheeswaran, M. Rajagopalan, J. Alloys Comp. 352 (2003) 60–65.
[13] K. Kusaba, T. Kikegawa, Solid State Commun. 148 (2008) 440–443.
[14] X.W. Sun, T. Song, Z.J. Liu, C.R. Zhang, J.H. Tian, P. Guo, Solid State Commun. 151 (2011) 1507–1510.
[15] H. Öztürk, C. Kürkçü, C. Kürkçü, J. Alloys Comp. 597 (2014) 155–160.
[16] Y.A. Nga, C.K. Ong, J. Chem. Phys. 98 (1993) 3240–3245.
[17] L.C. Ming, M.H. Manghnani, Geophys. Res. Lett. 6 (1979) 13–16.
[18] N.L. Allan, R.I. Hines, M.D. Towler, W.C. Mackrodt, J. Chem. Phys. 100 (1994) 4710–4711.
[19] K. Nishidate, M. Baba, T. Sato, K. Nishikawa, Phys. Rev. B 52 (1995) 3170–3176.
[20] G.D. Barrera, M.B. Taylor, N.L. Allan, T.H.K. Barron, L.N. Kantorovich, W.C. Mackrodt, J. Chem. Phys. 107 (1997) 4337–4344.
[21] E. Francisco, J.M. Recio, M.A. Blanco, A. Martin Pendas, A. Costales, J. Phys. Chem. A 102 (1998) 1595–1601.
[22] J.P. Perdew, K. Burke, M. Ernzerhof, Phys. Rev. Lett. 77 (1996) 3865–3868.
[23] P. Ordejon, E. Artacho, J.M. Soler, Phys. Rev. B 53 (R10) (1996) 441–444.
[24] N. Troullier, J.L. Martins, Phys. Rev. B 43 (1991) 1993–2006.
[25] M. Durandurdu, D.A. Drabold, Phys. Rev. B 66 (2002). 045209-1-5.
[26] M. Özduran, M. Durandurdu, Eur. Phys. Lett. 84 (2008). 56001-1-4.
[27] S. Eker, M. Durandurdu, Eur. Phys. Lett. 87 (2009). 36001-1-5.
[28] H. Öztürk, M. Durandurdu, Phys. Rev. B 79 (2009). 134111-1-6.
[29] S. Alptekin, M. Durandurdu, Solid State Commun. 150 (2010) 870–874.
[30] H. Ozturk, M. Durandurdu, J. Am. Ceram. Soc. 94 (2011) 932–937.
[31] A. Hannemann, R. Hundt, J.C. Schön, M. Jansen, J. Appl. Cryst. 31 (1998) 922–928.
[32] R. Hundt, J.C. Schön, A. Hannemann, M. Jansen, J. Appl. Crys. 32 (1999) 413–416.
[33] H.J. Monkhorst, J.D. Pack, Phys. Rev. B 13 (1976) 5188–5192.
[34] F. Birch, Phys. Rev. 71 (1947) 809–824.
[35] F.D. Murnaghan, Proc. Natl. Acad. Sci. USA 30 (1944) 244–247.
[36] K. Mizushima, S. Yip, E. Kaxiras, Phys. Rev. B 50 (1994) 14952–14959.
[37] R. Martonak, A. Laio, M. Parrinello, Phys. Rev. Lett. 90 (2003). 075503-1-4.
[38] L. Zhang, Y. Wang, T. Cui, Y. Ma, G. Zou, Solid State Commun. 145 (2008) 283–287.